

lecture 14

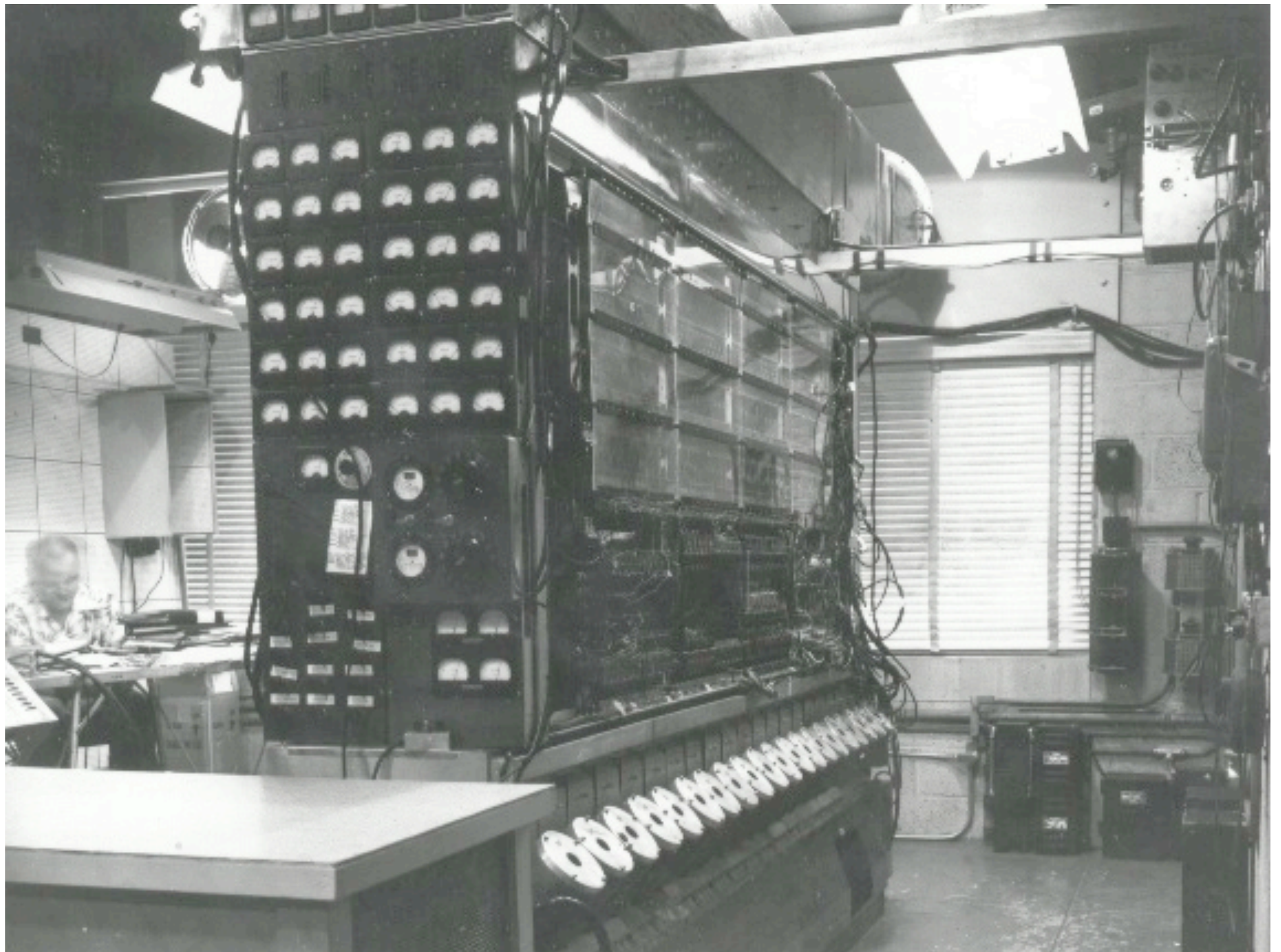
Climate Change Modeling

DEVELOPMENT OF EARTH SYSTEM MODELS

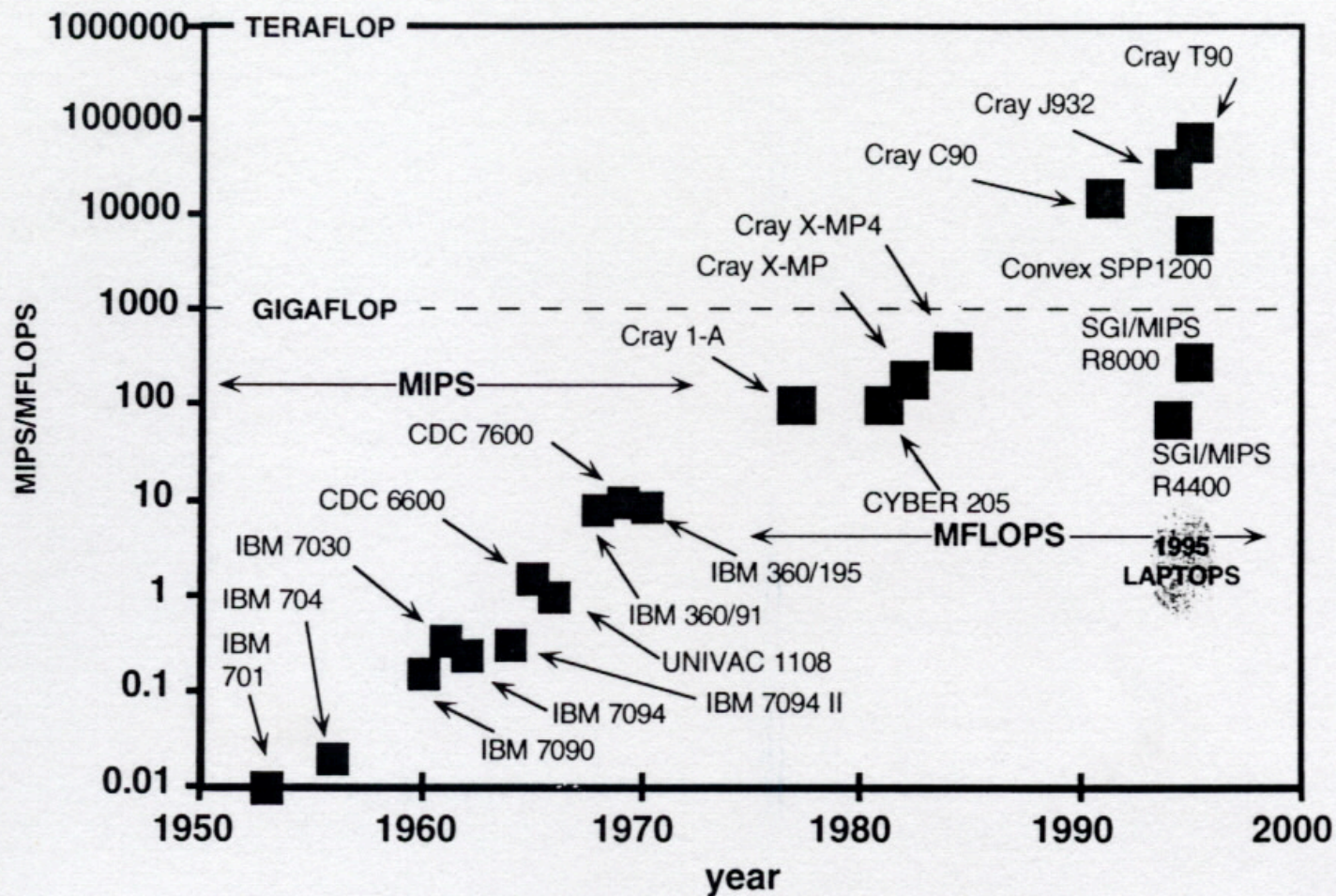
Lewis Richardson (1881-1953)

In the 1920s, he proposed solving the weather prediction equations using numerical methods. Worked for six weeks to do a six-hour “hindcast” by hand. Proposed a wild scheme to predict the weather in real time. His scheme was totally impractical because of the lack of computing power.

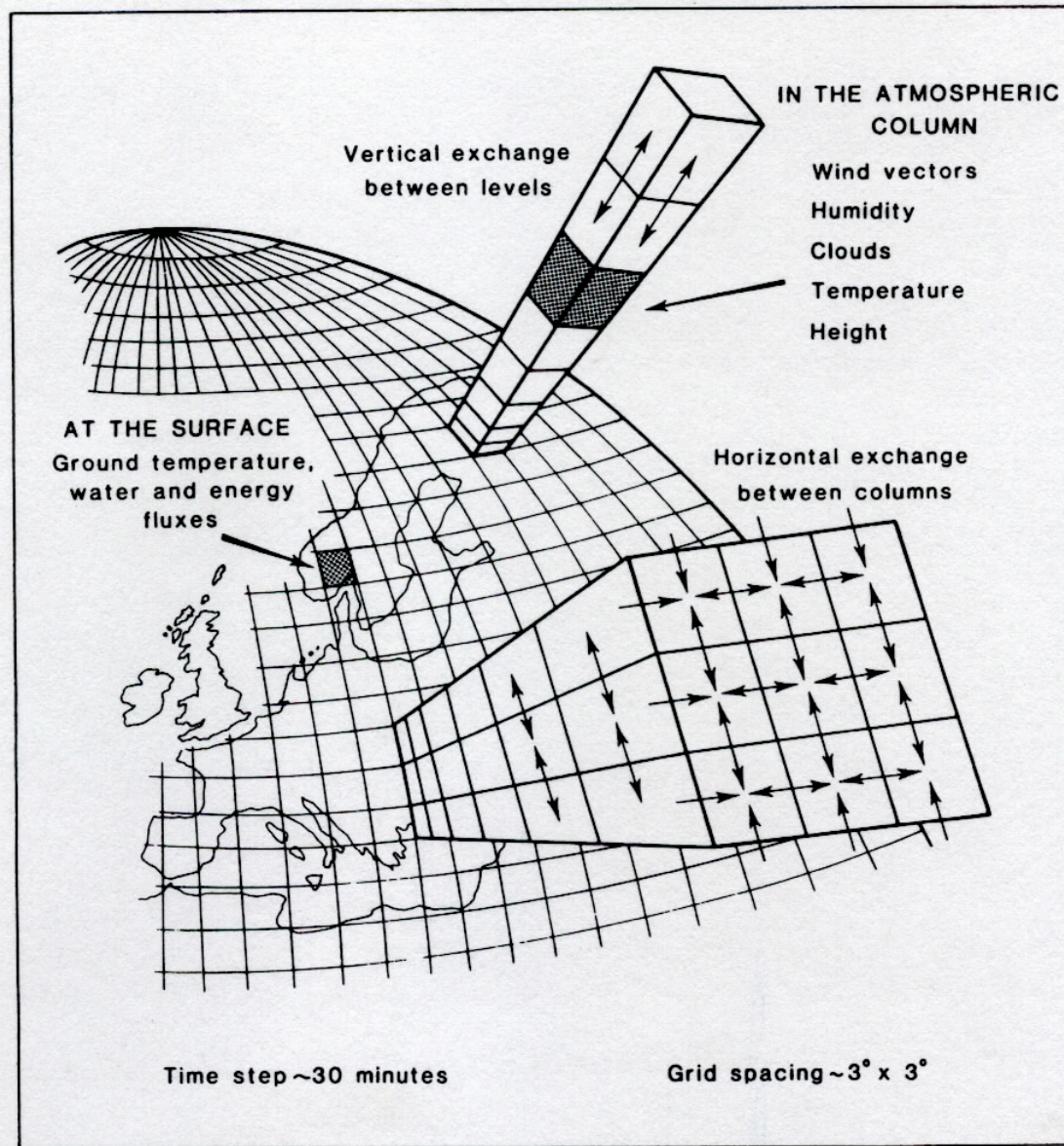




Over the past 50 years, there has been a remarkable increase in computing power, which has facilitated the development of numerical models to study weather and climate. We call these **general circulation models (GCMs)**.

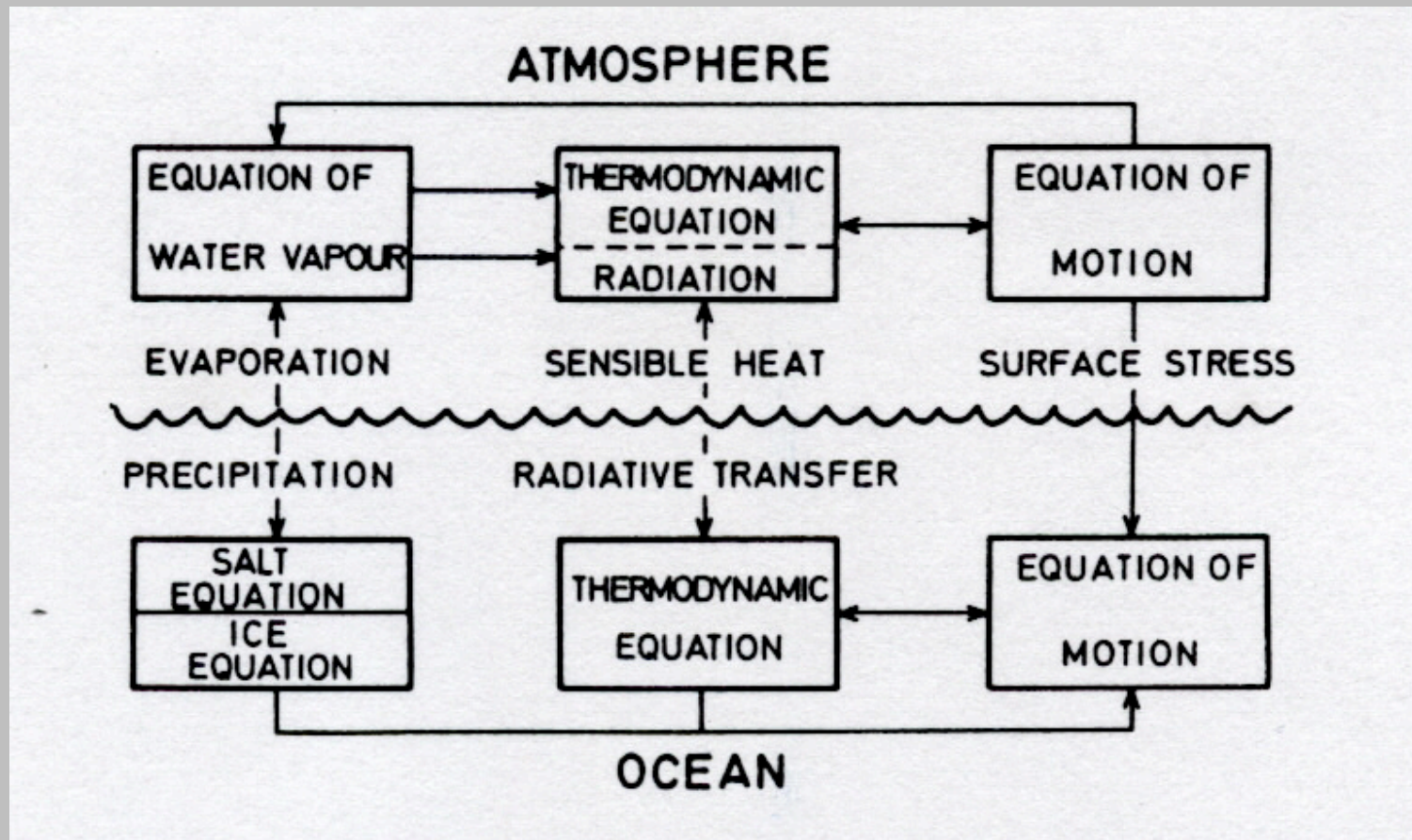


Computational grid of a general circulation model

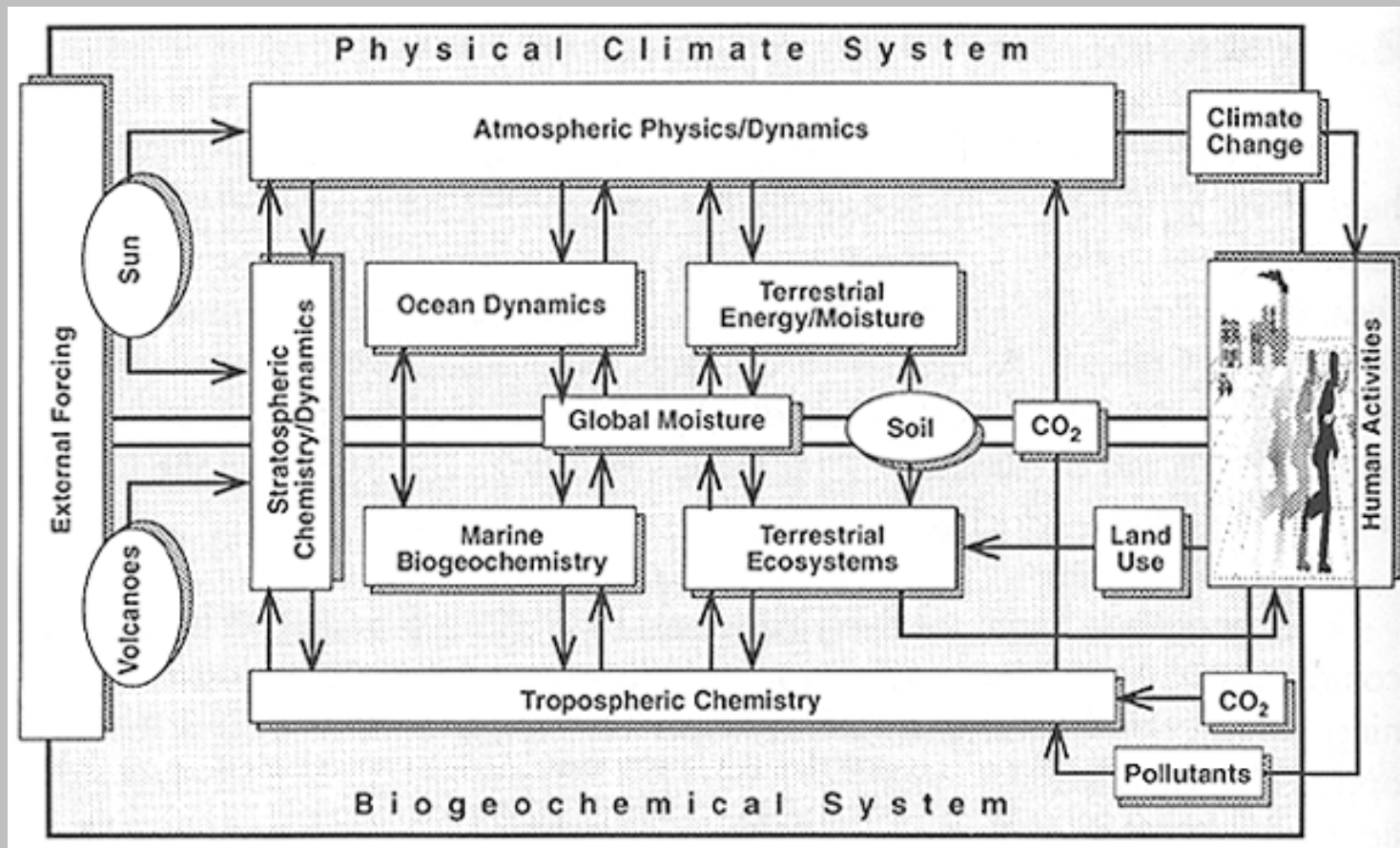


This is the typical resolution of a climate model. Note that there are many important processes for climate that cannot be resolved explicitly on such a coarse grid.

structure of a climate model (GCM)



towards an earth system model



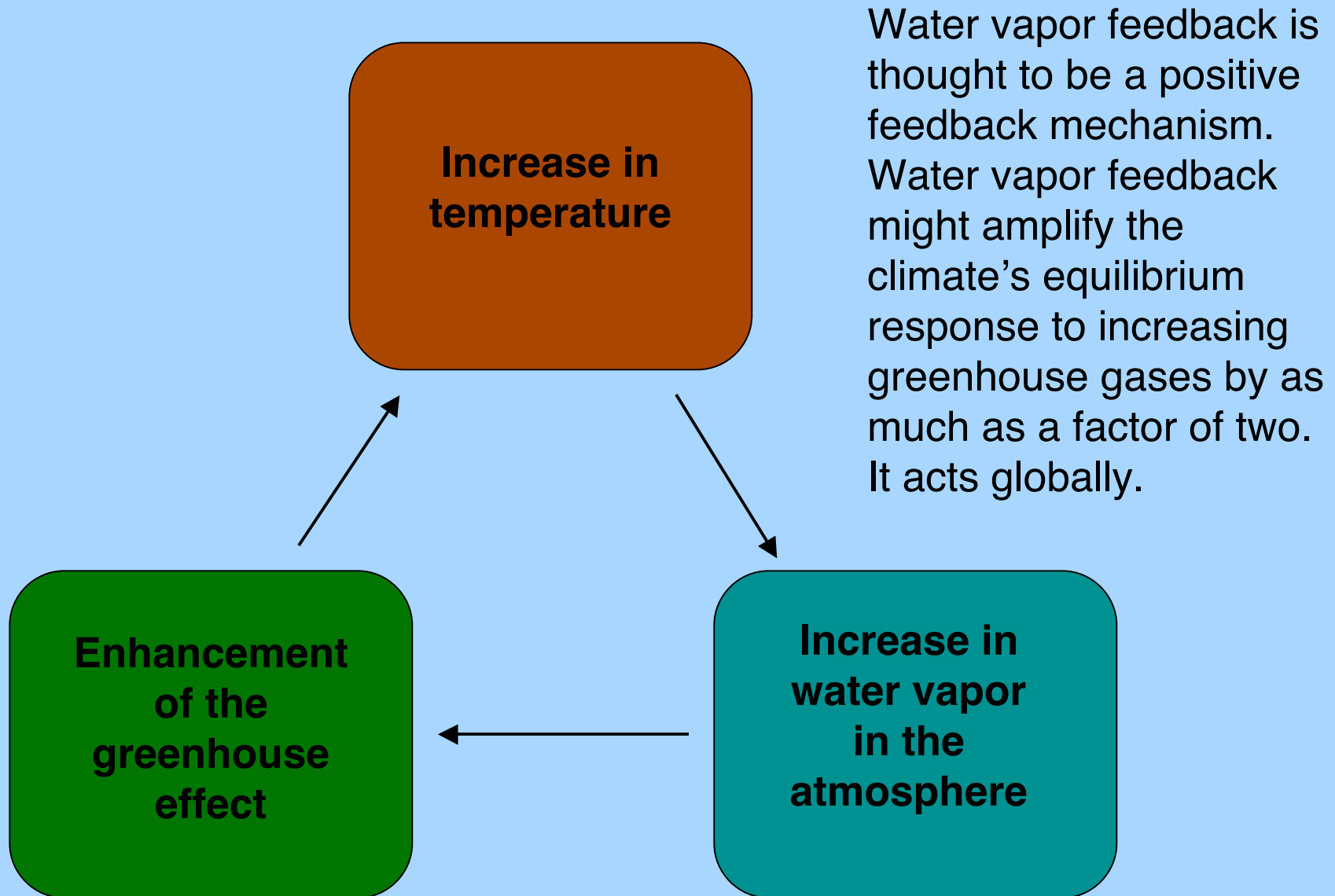
Source: *Earth System Science: Overview*, NASA

CLIMATE FEEDBACKS

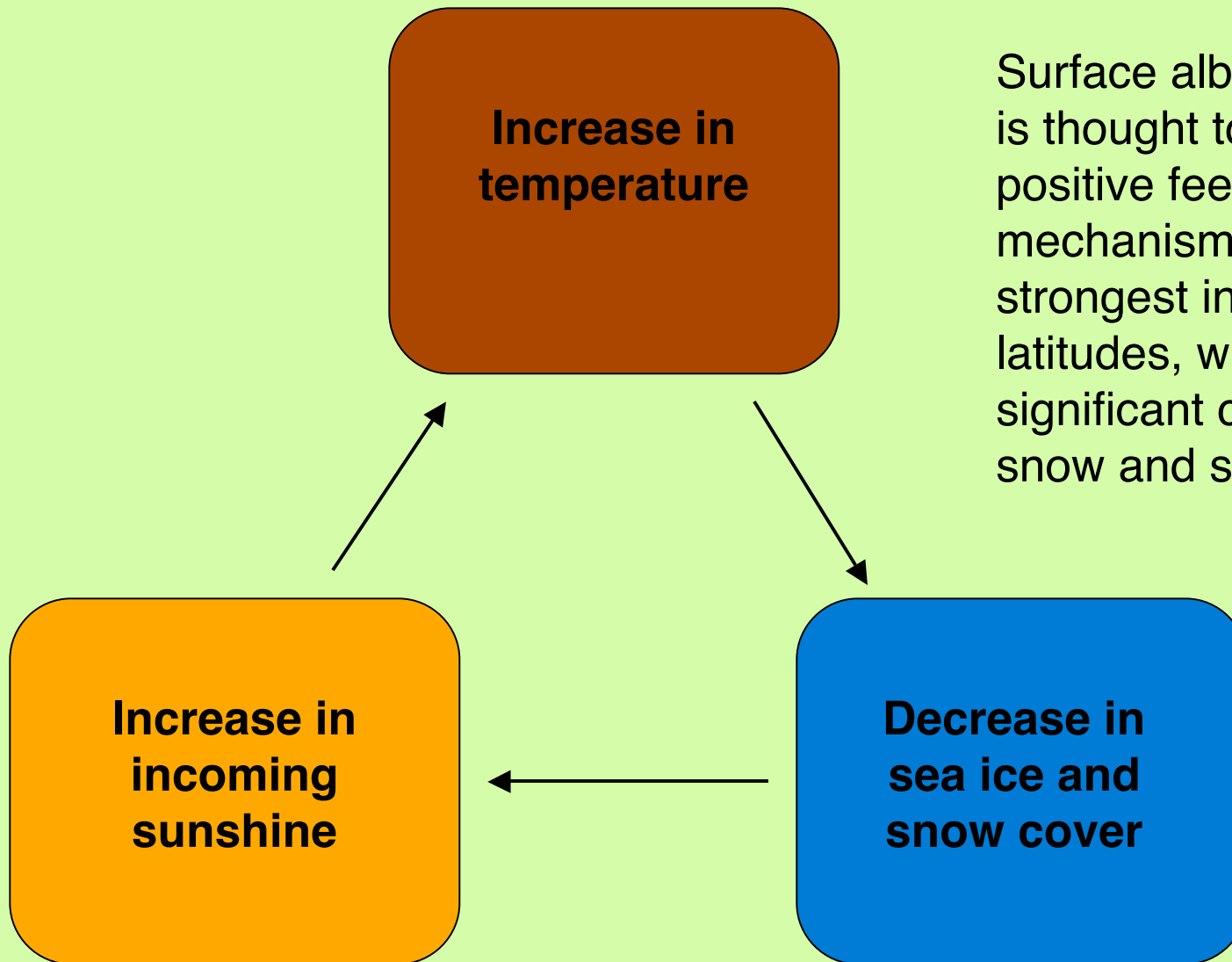
If the climate's response to an increase in greenhouse gases were simply to increase its temperature to compensate for the increase in greenhouse trapping of infrared radiation, the climate change problem would be quite simple. Unfortunately, there are climate feedbacks that come into play, influencing the climate's response. The main climate feedbacks are:

- (1) Water vapor feedback**
- (2) Surface albedo feedback**
- (3) Cloud feedback**

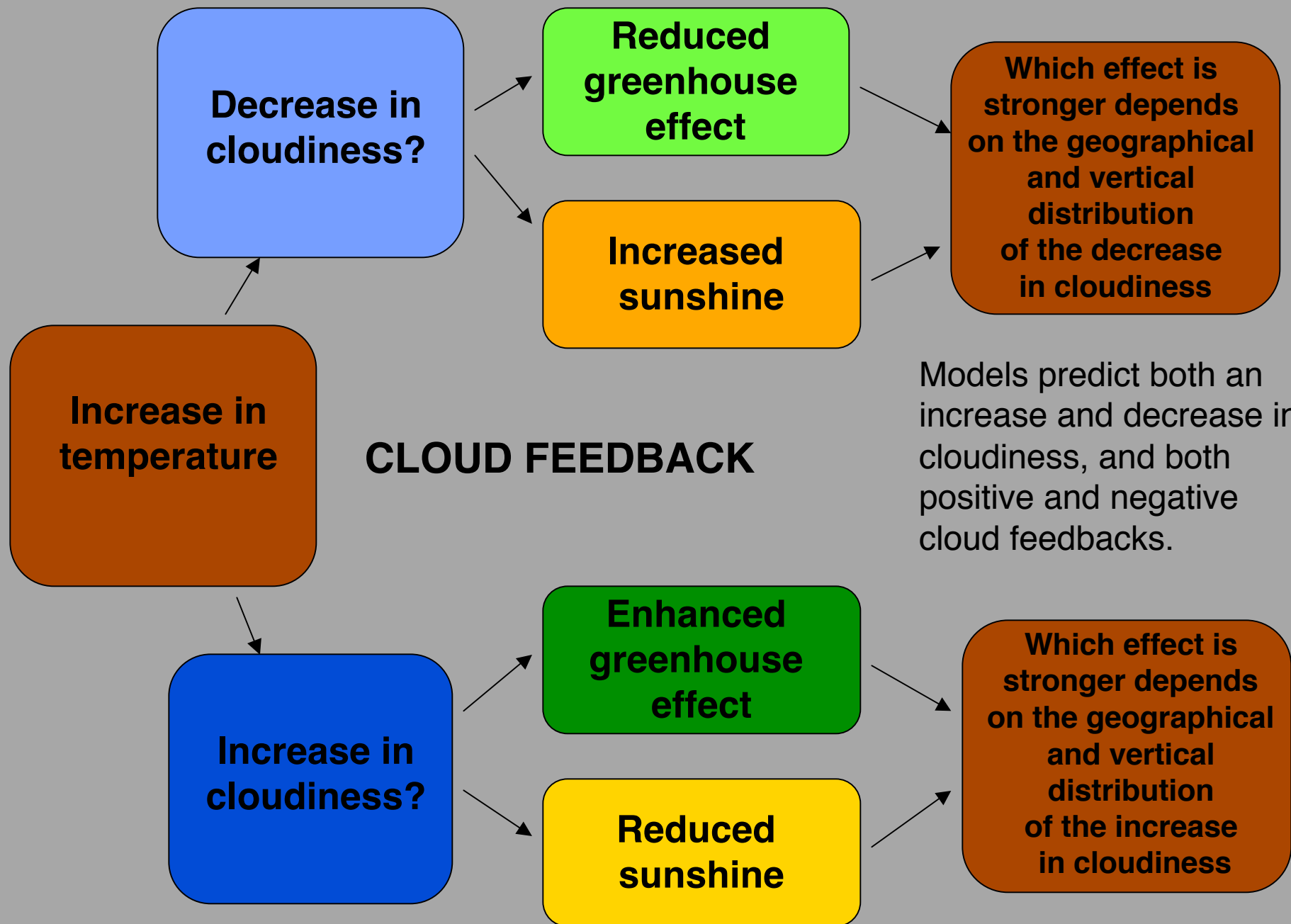
WATER VAPOR FEEDBACK



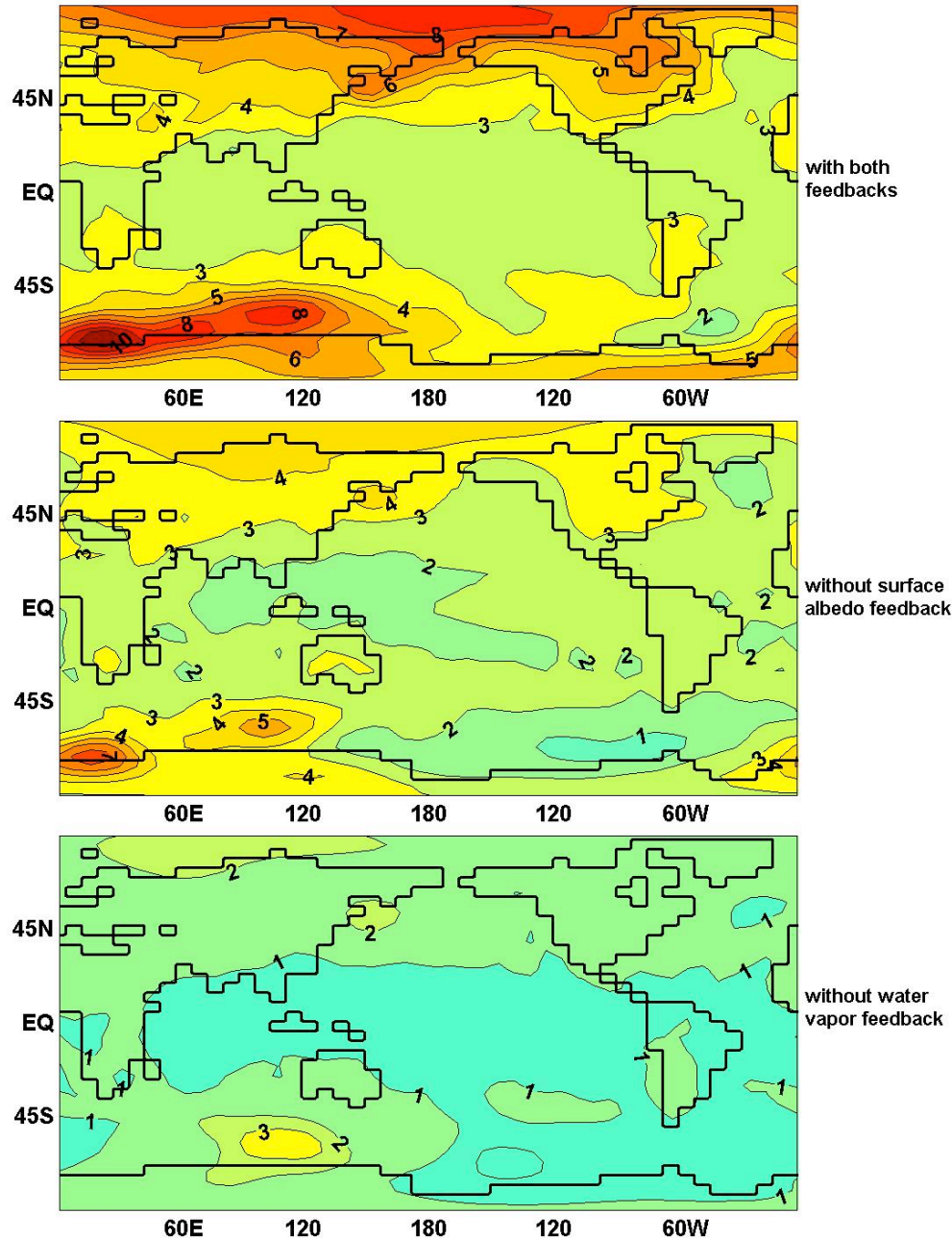
SURFACE ALBEDO FEEDBACK



Surface albedo feedback is thought to be a positive feedback mechanism. Its effect is strongest in mid to high latitudes, where there is significant coverage of snow and sea ice.



Effect of water vapor and surface albedo feedbacks on the quasi-equilibrium SAT increase due to CO₂-doubling in a coupled ocean-atmosphere model



Equilibrium response of a climate model when feedbacks are removed.

If the forcing associated with a doubling of CO₂ is approximately 4 W/m², what is the approximate sensitivity of each model on a global-mean basis?

To calculate the climate sensitivity, we divide the response by the forcing.

IDEALIZED RESPONSE OF MODELS TO EXTERNAL FORCING

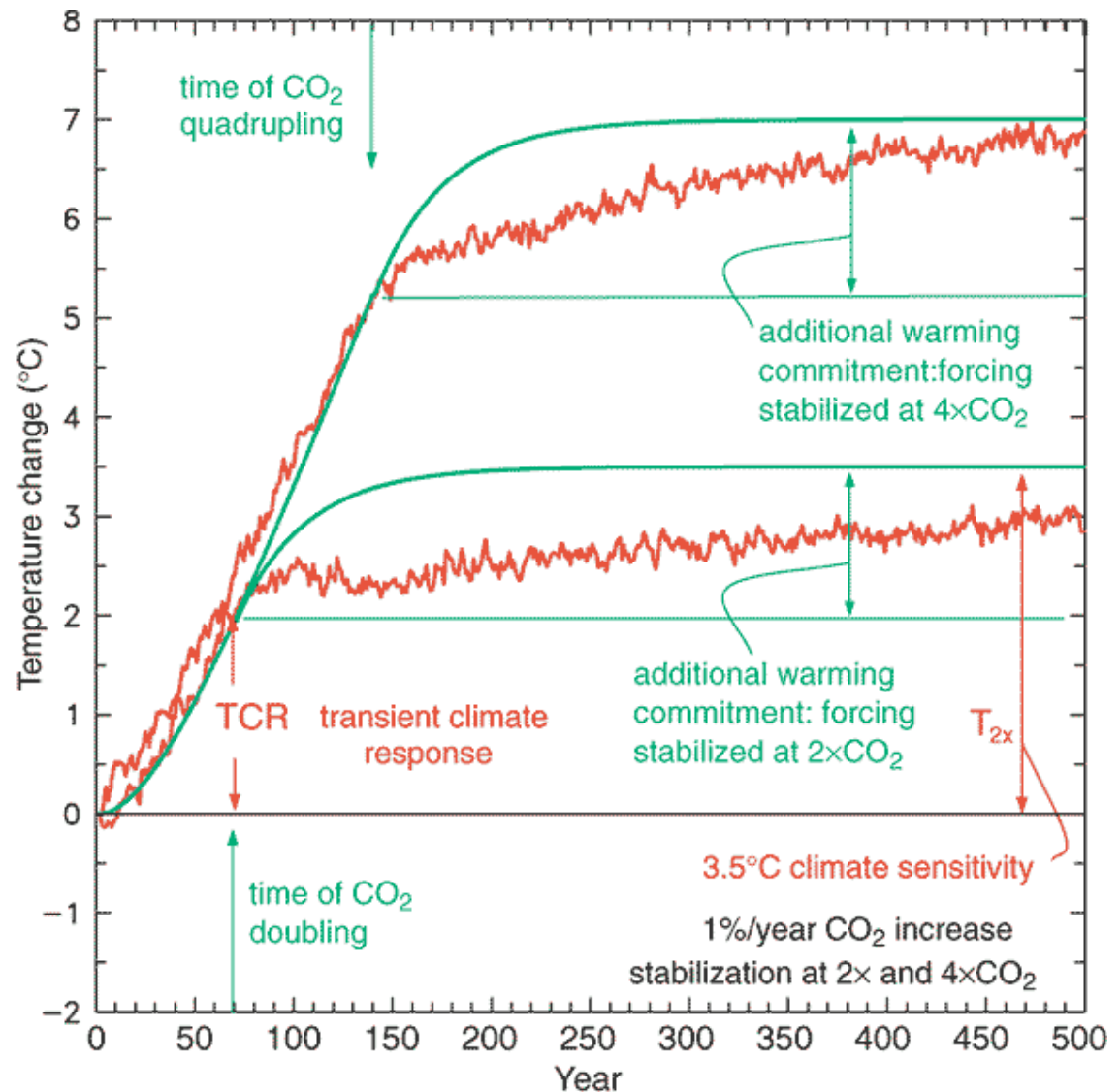
Transient vs Equilibrium climate response

Transient response refers to the evolution of the climate system as it responds to external forcing, such as an increase in greenhouse gases.

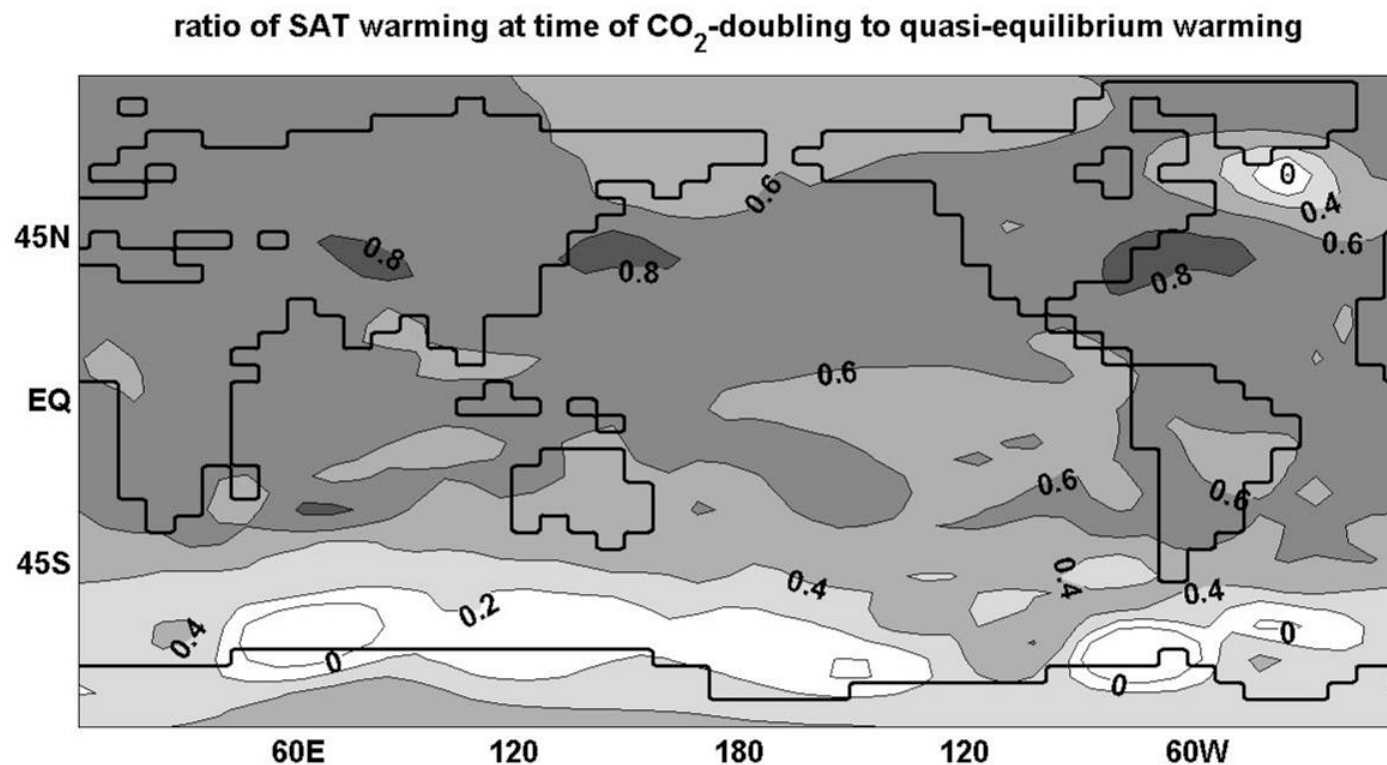
Equilibrium response refers to the final state of the climate system after it has adjusted to the external forcing. The magnitude of the equilibrium response compared to the magnitude of the forcing is referred to as the **climate sensitivity**.

Evolution of simulated global mean temperature when CO₂ changes

This shows the warming in a climate model when two scenarios of CO₂ increases are imposed: one is a 1% per year increase in CO₂ leading to a CO₂ doubling, and the other is an increase at the same rate leading to a CO₂ quadrupling. It shows that the warming continues for several centuries even when CO₂ levels are stabilized, leading to significant differences between transient and equilibrium climate responses to external forcing.



The difference between the transient and equilibrium responses of a climate model to increasing greenhouse gases vary a great deal geographically. Which parts of the world take the longest to equilibrate to the external forcing?



ATTRIBUTION OF CLIMATE CHANGE

GLOBAL MEAN SURFACE TEMPERATURE ANOMALIES

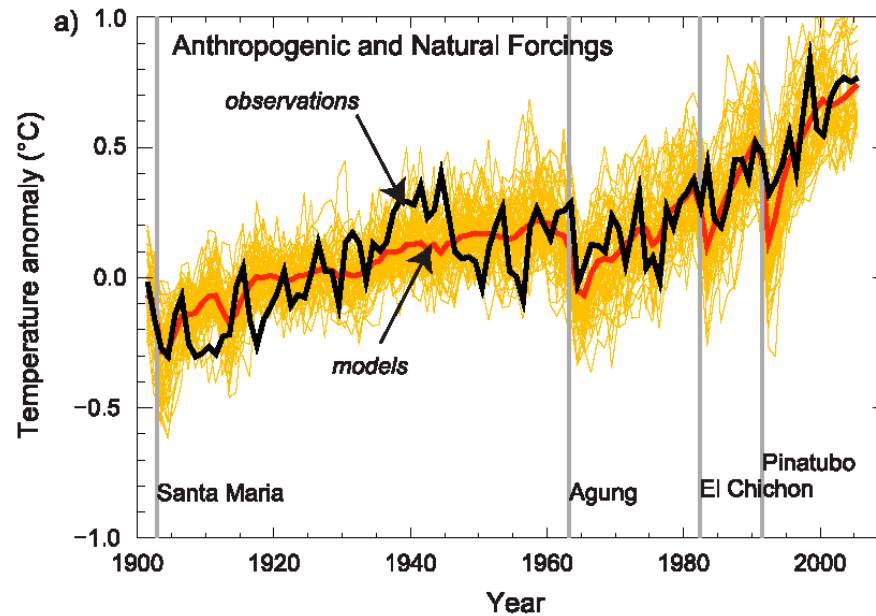
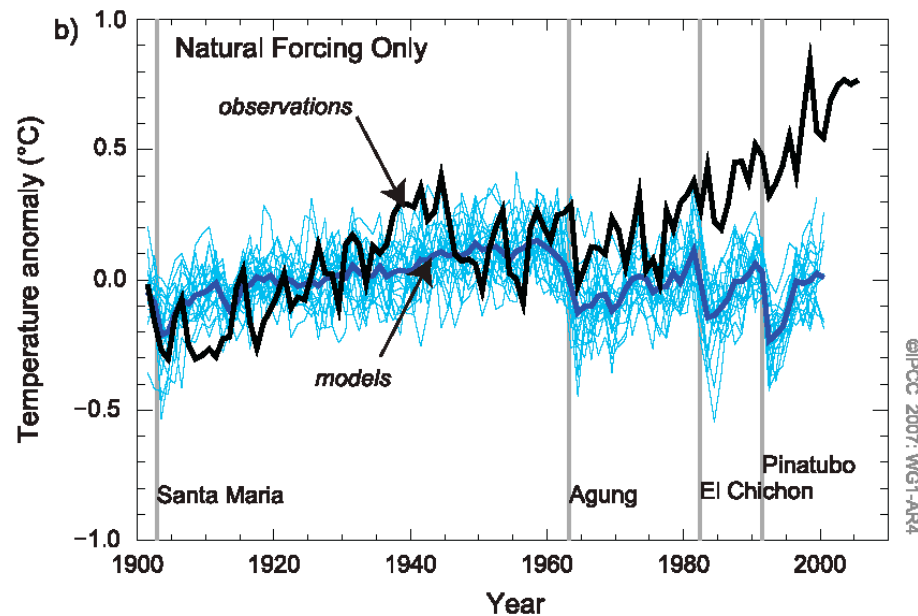
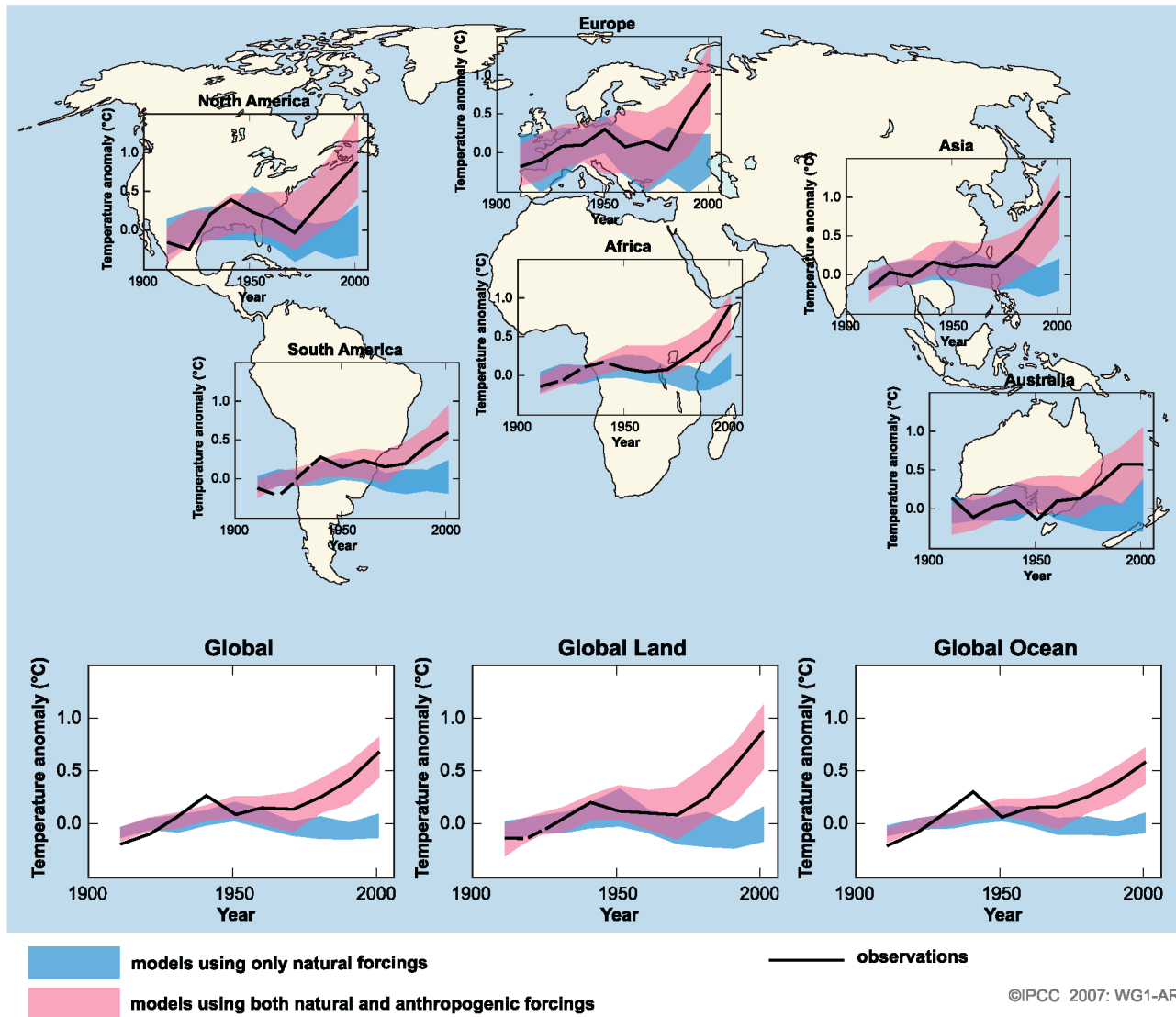


Figure TS.23. (a) Global mean surface temperature anomalies relative to the period 1901 to 1950, as observed (black line) and as obtained from simulations with both anthropogenic and natural forcings. The thick red curve shows the multi-model ensemble mean and the thin yellow curves show the individual simulations. Vertical grey lines indicate the timing of major volcanic events. (b) As in (a), except that the simulated global mean temperature anomalies are for natural forcings only. The thick blue curve shows the multi-model ensemble mean and the thin lighter blue curves show individual simulations. Each simulation was sampled so that coverage corresponds to that of the observations. {Figure 9.5}

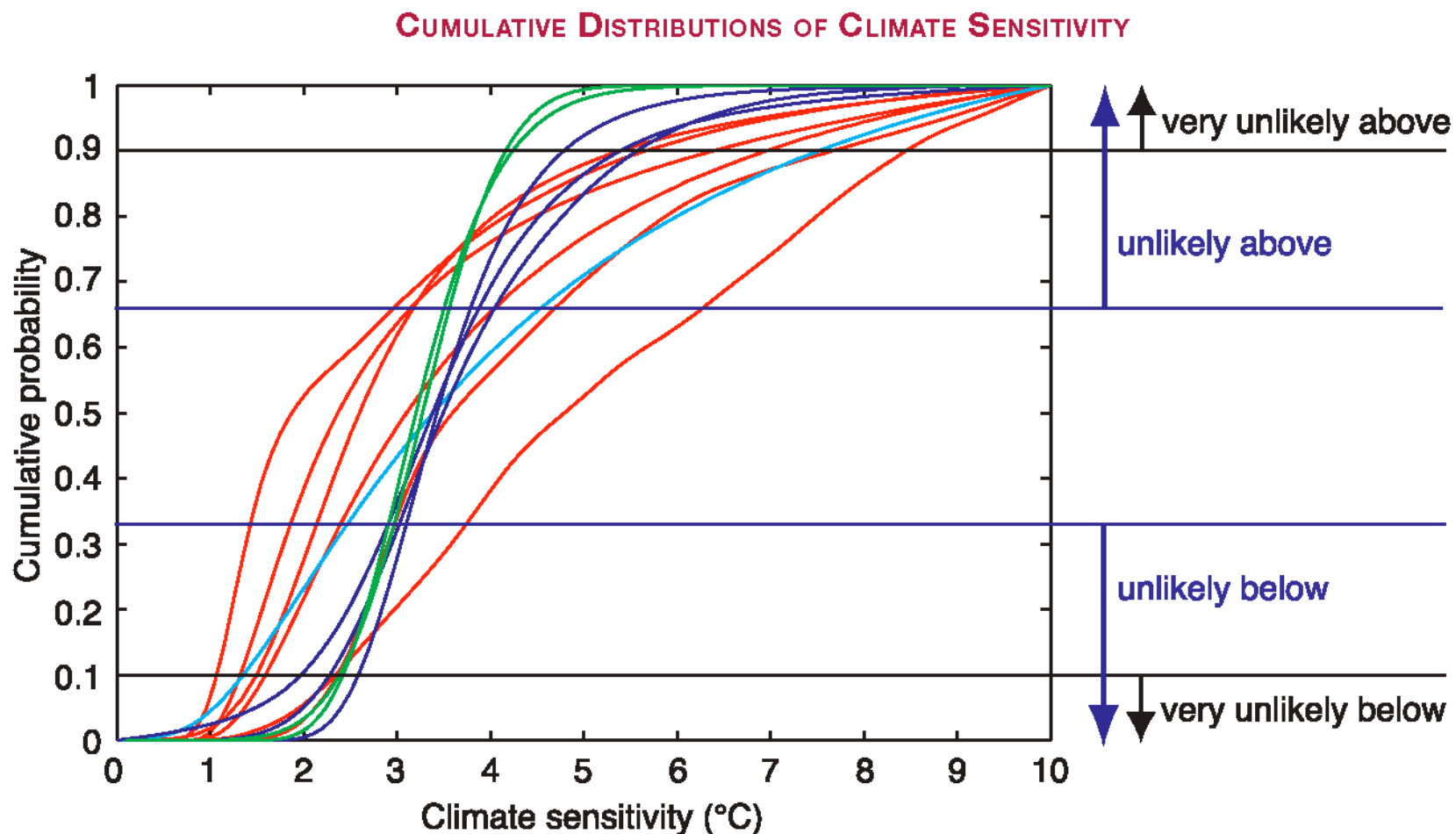


GLOBAL AND CONTINENTAL TEMPERATURE CHANGE



©IPCC 2007: WG1-AR4

Figure TS.22. Comparison of observed continental- and global-scale changes in surface temperature with results simulated by climate models using natural and anthropogenic forcings. Decadal averages of observations are shown for the period 1906 to 2005 (black line) plotted against the centre of the decade and relative to the corresponding average for 1901 to 1950. Lines are dashed where spatial coverage is less than 50%. Blue shaded bands show the 5% to 95% range for 19 simulations from 5 climate models using only the natural forcings due to solar activity and volcanoes. Red shaded bands show the 5% to 95% range for 58 simulations from 14 climate models using both natural and anthropogenic forcings. Data sources and models used are described in Section 9.4, FAQ 9.2, Table 8.1 and the supplementary information for Chapter 9. {FAQ 9.2, Figure 1}

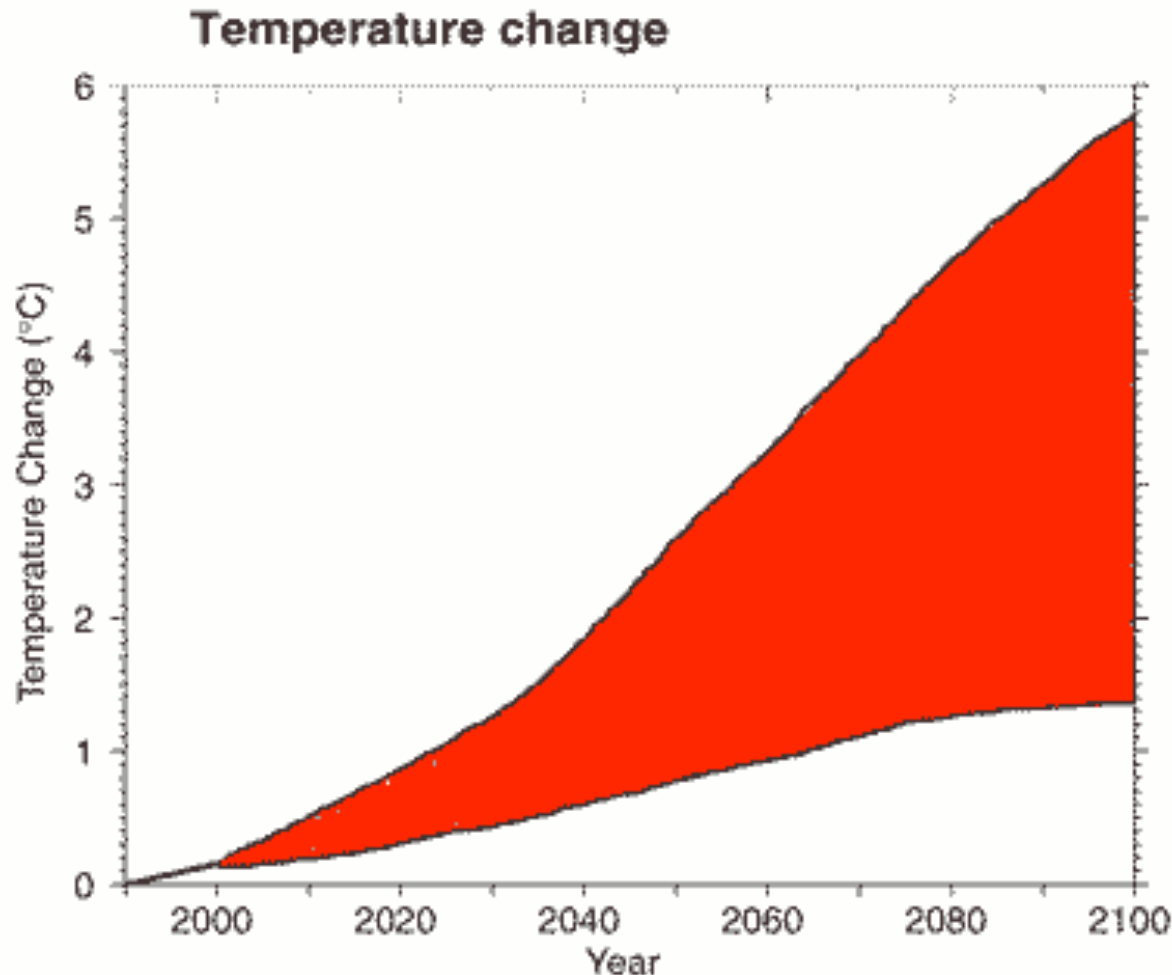


©IPCC 2007: WG1-AR4

Figure TS.25. Cumulative distributions of climate sensitivity derived from observed 20th-century warming (red), model climatology (blue), proxy evidence (cyan) and from climate sensitivities of AOGCMs (green). Horizontal lines and arrows mark the boundaries of the likelihood estimates defined in the IPCC Fourth Assessment Uncertainty Guidance Note (see Box TS.1). {Box 10.2, Figures 1 and 2}

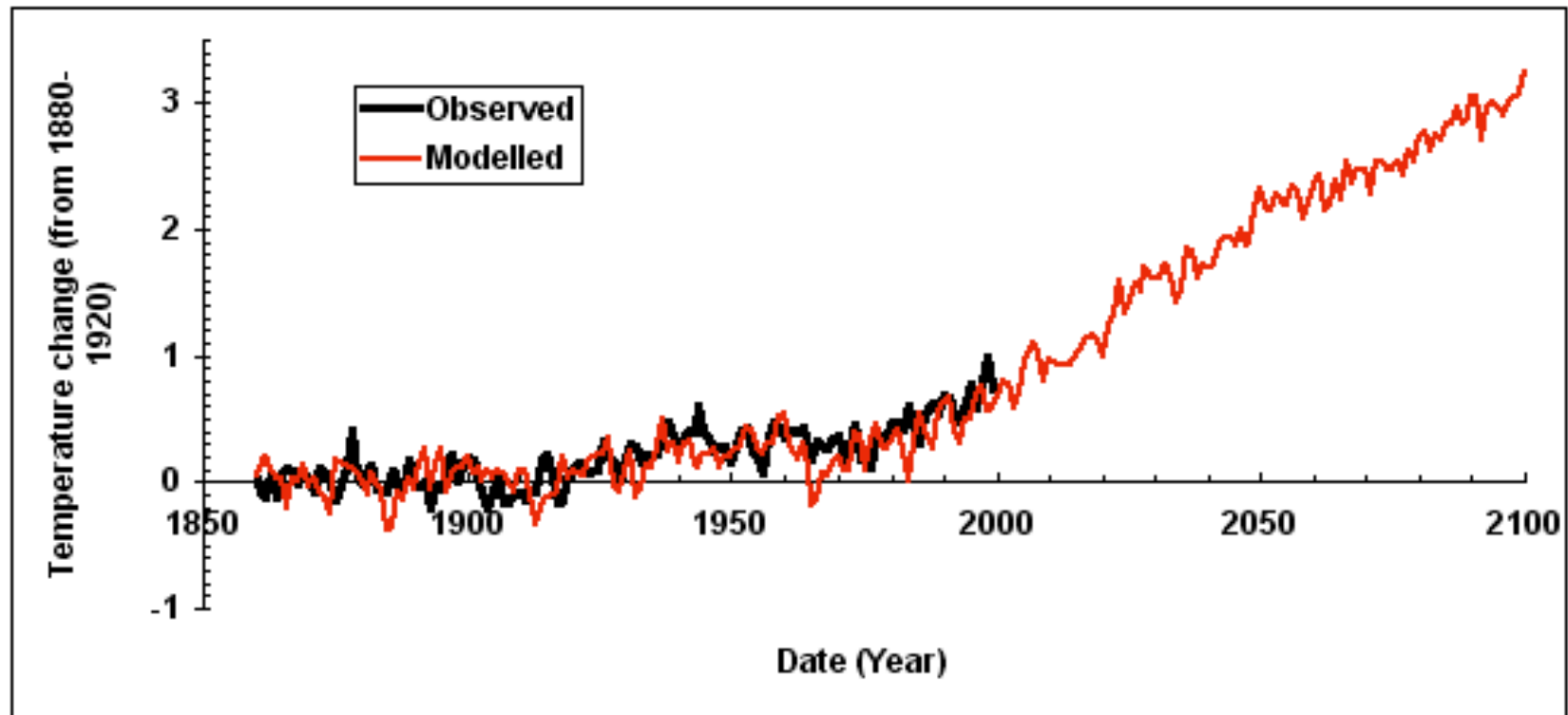
PREDICTIONS OF FUTURE CLIMATE

Uncertainty about the future: This plot shows the upper and lower limits of the global mean warming over the coming century predicted by current GCM simulations.



This range is due to two factors: (1) uncertainty in emissions scenarios and (2) different model sensitivities (i.e. different simulations of climate feedbacks).

We can also impose realistic forcing scenarios to see how well climate simulations reproduce the observed climate record. When our best guess of the observed increase in greenhouse gases and sulfate aerosols is imposed on a general circulation model, the model simulates the warming trend over the past century quite well. Note that the warming trend over the next century is projected to dwarf that of the past century. This particular model was developed at the Hadley Centre in the U.K.



GLOBAL MEAN WARMING: MODEL PROJECTIONS COMPARED WITH OBSERVATIONS

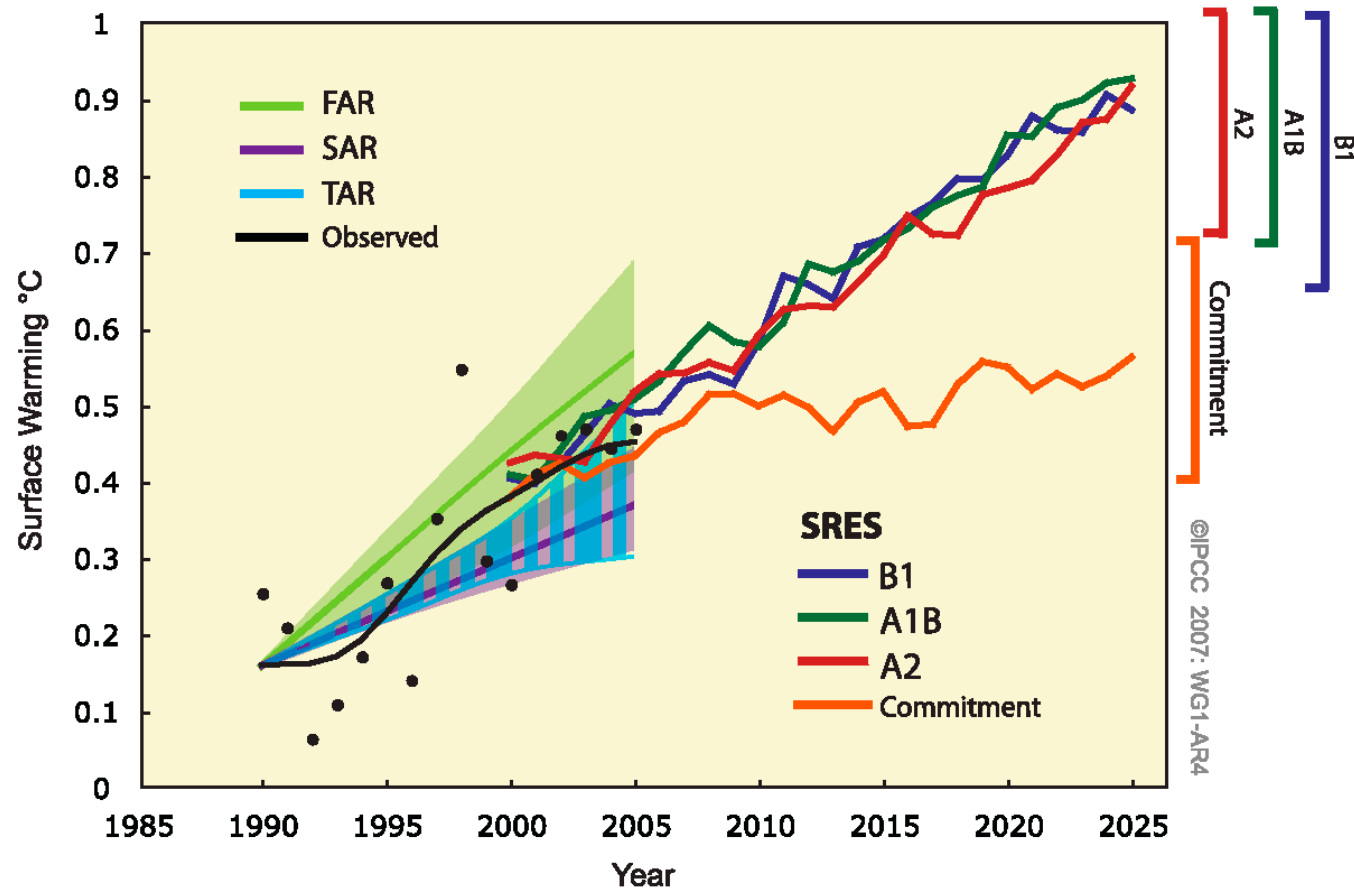


Figure TS.26. Model projections of global mean warming compared to observed warming. Observed temperature anomalies, as in Figure TS.6, are shown as annual (black dots) and decadal average values (black line). Projected trends and their ranges from the IPCC First (FAR) and Second (SAR) Assessment Reports are shown as green and magenta solid lines and shaded areas, and the projected range from the TAR is shown by vertical blue bars. These projections were adjusted to start at the observed decadal average value in 1990. Multi-model mean projections from this report for the SRES B1, A1B and A2 scenarios, as in Figure TS.32, are shown for the period 2000 to 2025 as blue, green and red curves with uncertainty ranges indicated against the right-hand axis. The orange curve shows model projections of warming if greenhouse gas and aerosol concentrations were held constant from the year 2000 – that is, the committed warming. (Figures 1.1 and 10.4)

Table TS.6. *Projected global average surface warming and sea level rise at the end of the 21st century. {10.5, 10.6, Table 10.7}*

Case	Temperature Change (°C at 2090-2099 relative to 1980-1999) ^a		Sea Level Rise (m at 2090-2099 relative to 1980-1999)
	Best estimate	Likely range	Model-based range excluding future rapid dynamical changes in ice flow
Constant Year 2000 concentrations ^b	0.6	0.3 – 0.9	NA
B1 scenario	1.8	1.1 – 2.9	0.18 – 0.38
A1T scenario	2.4	1.4 – 3.8	0.20 – 0.45
B2 scenario	2.4	1.4 – 3.8	0.20 – 0.43
A1B scenario	2.8	1.7 – 4.4	0.21 – 0.48
A2 scenario	3.4	2.0 – 5.4	0.23 – 0.51
A1FI scenario	4.0	2.4 – 6.4	0.26 – 0.59

Notes:

^a These estimates are assessed from a hierarchy of models that encompass a simple climate model, several Earth Models of Intermediate Complexity (EMICs), and a large number of Atmosphere-Ocean Global Circulation Models (AOGCMs).

^b Year 2000 constant composition is derived from AOGCMs only.

PROJECTIONS OF SURFACE TEMPERATURES

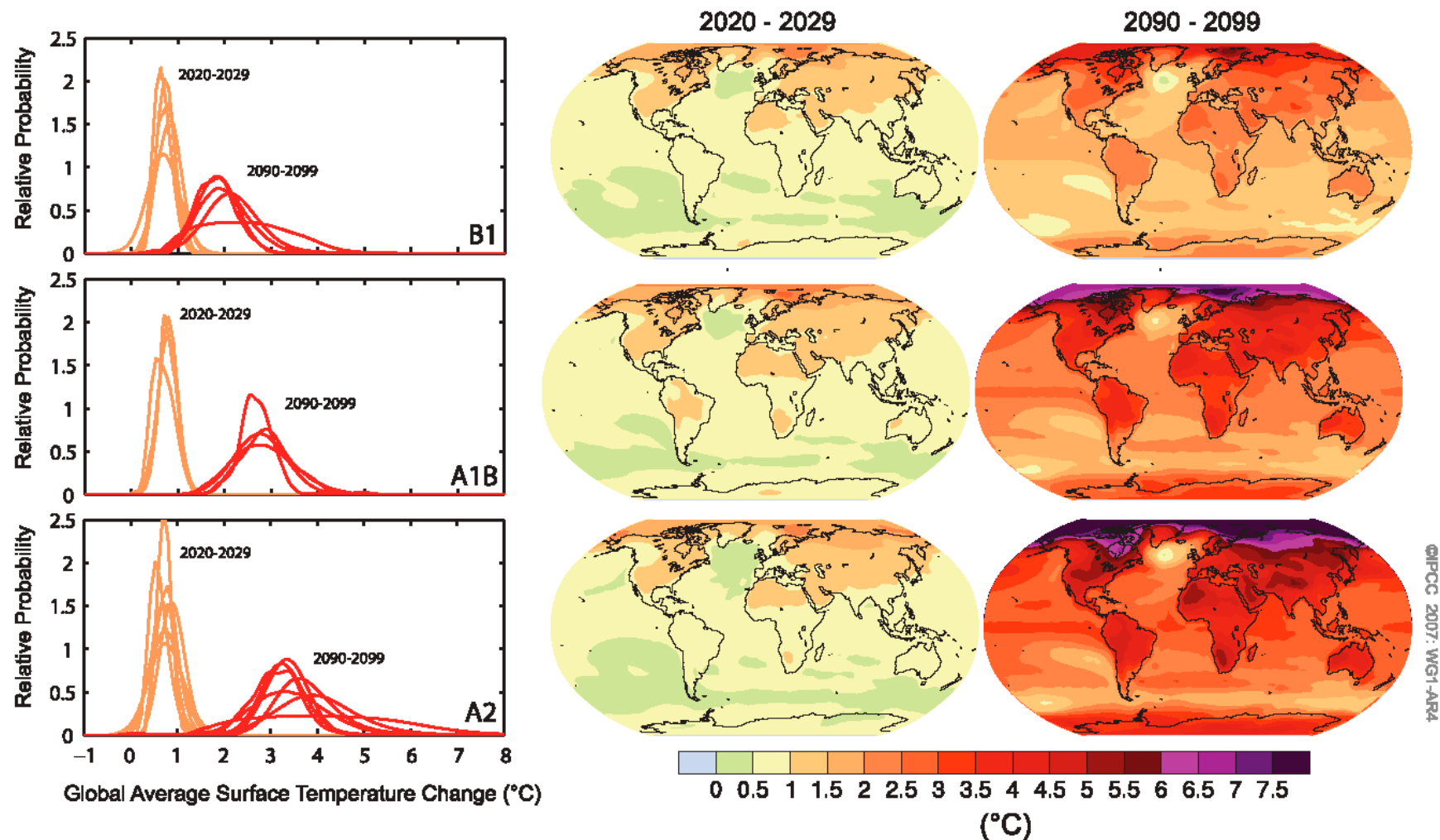
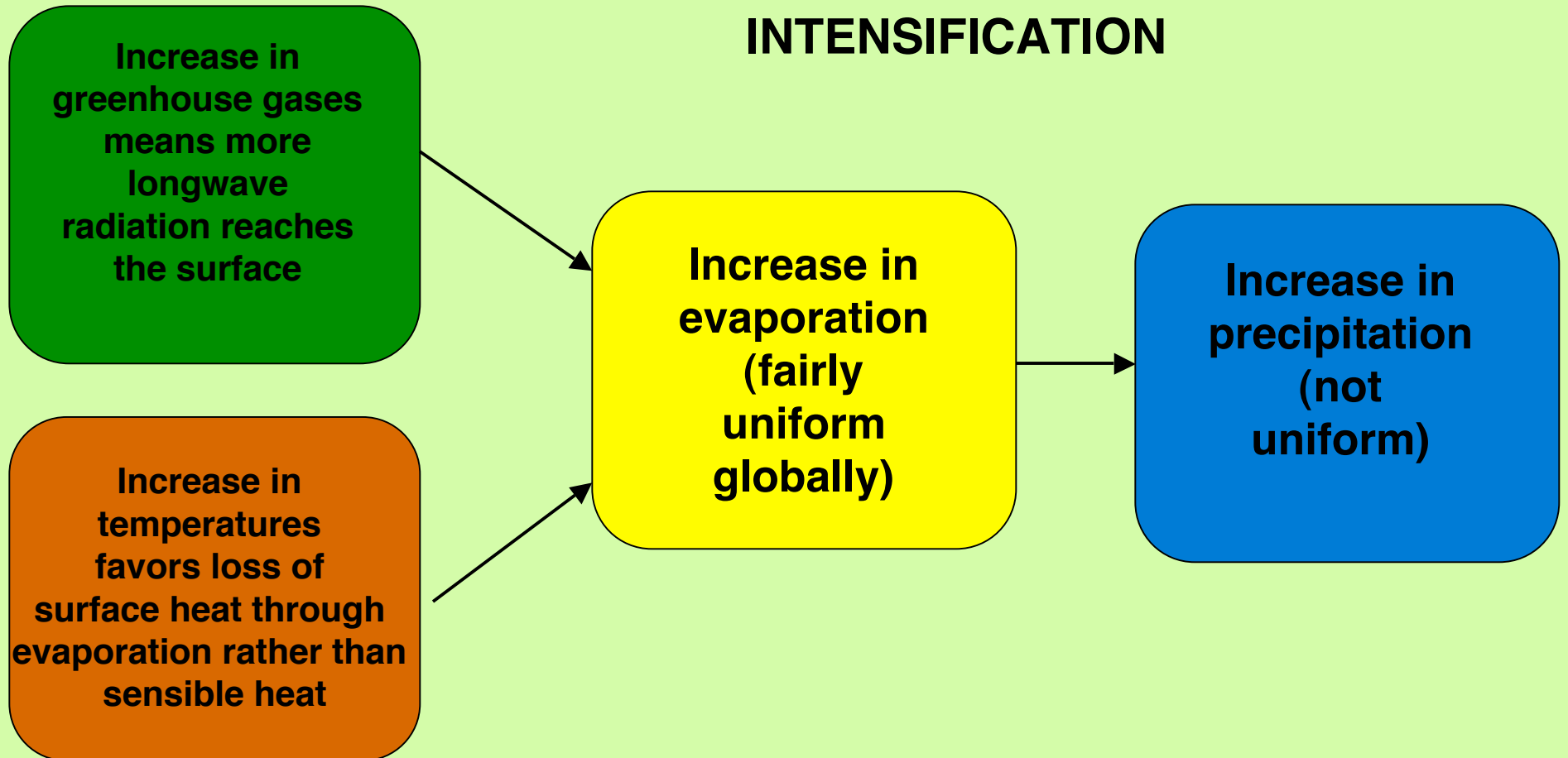


Figure TS.28. Projected surface temperature changes for the early and late 21st century relative to the period 1980 to 1999. The central and right panels show the AOGCM multi-model average projections ($^{\circ}\text{C}$) for the B1 (top), A1B (middle) and A2 (bottom) SRES scenarios averaged over the decades 2020 to 2029 (centre) and 2090 to 2099 (right). The left panel shows corresponding uncertainties as the relative probabilities of estimated global average warming from several different AOGCM and EMIC studies for the same periods. Some studies present results only for a subset of the SRES scenarios, or for various model versions. Therefore the difference in the number of curves, shown in the left-hand panels, is due only to differences in the availability of results. {Adapted from Figures 10.8 and 10.28}

HYDROLOGIC CYCLE INTENSIFICATION



SEASONAL MEAN PRECIPITATION RATES

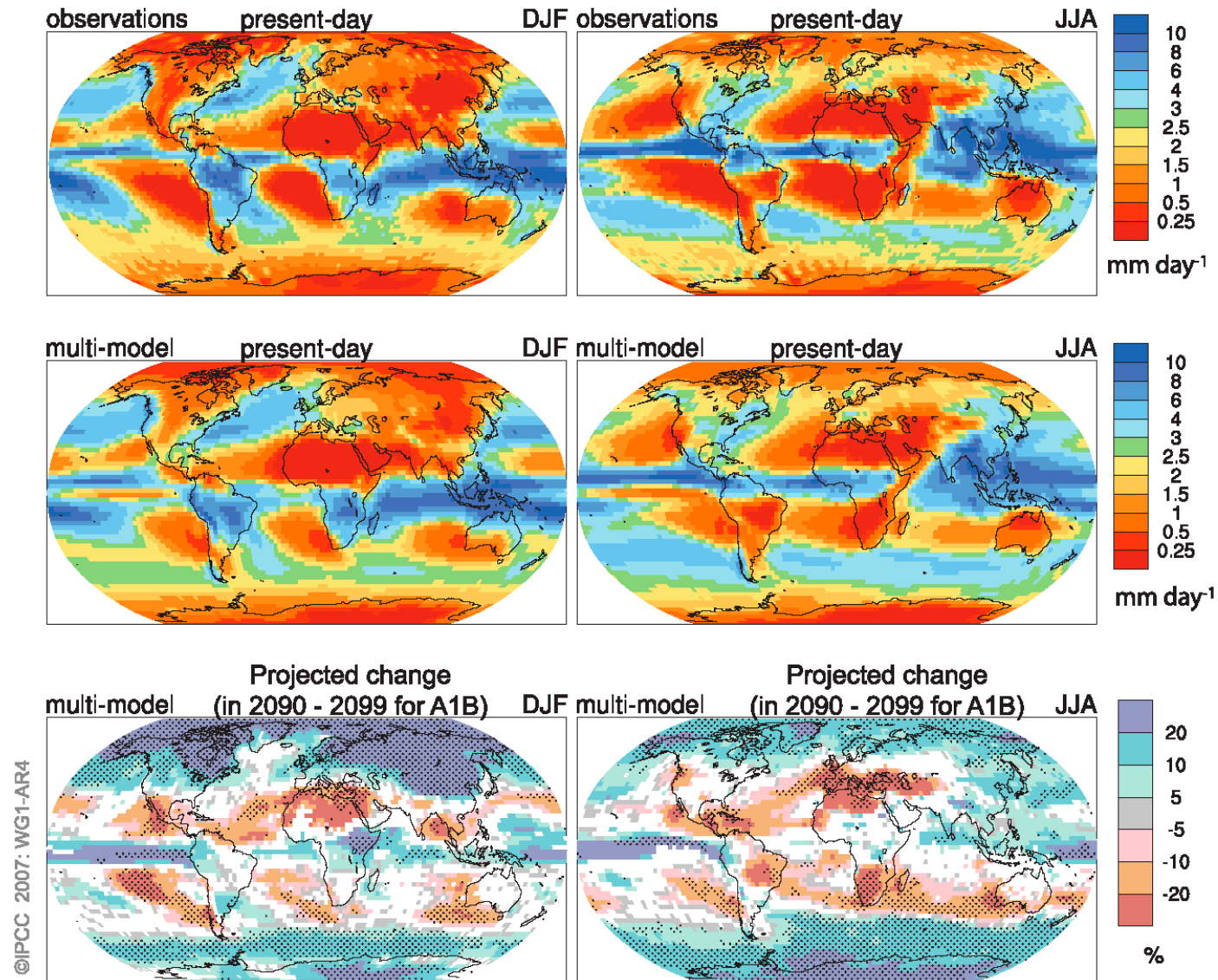


Figure TS.30. Spatial patterns of observed (top row) and multi-model mean (middle row) seasonal mean precipitation rate (mm day^{-1}) for the period 1979 to 1993 and the multi-model mean for changes by the period 2090 to 2099 relative to 1980 to 1999 (% change) based on the SRES A1B scenario (bottom row). December to February means are in the left column, June to August means in the right column. In the bottom panel, changes are plotted only where more than 66% of the models agree on the sign of the change. The stippling indicates areas where more than 90% of the models agree on the sign of the change. {Based on same datasets as shown in Figures 8.5 and 10.9}